

Sequence divergence in the *Treponema denticola* FhbB protein and its impact on factor H binding

D.P. Miller¹, J.V. McDowell¹, D.V. Rhodes¹, A. Allard², M. Caimano², J.K. Bell³ and R.T. Marconi^{1,4}

¹ Department of Microbiology and Immunology, Medical College of Virginia at Virginia Commonwealth University, Richmond, VA, USA

² Department of Medicine, University of Connecticut Health Center, Farmington, CT, USA

³ Department of Biochemistry and Molecular Biology, Medical College of Virginia at Virginia Commonwealth University, Richmond, VA, USA

⁴ Center for the Study of Biological Complexity, Medical College of Virginia at Virginia Commonwealth University, Richmond, VA, USA

Correspondence: Richard T. Marconi, Department of Microbiology and Immunology, P.O. Box 980678, Virginia Commonwealth University, Richmond, VA 23298, USA Tel.: +1 804 828 3779; fax: +1 804 827 1310; E-mail: rmarconi@vcu.edu

Keywords: complement; factor H; immune evasion; periodontitis

Accepted 1 February 2013

DOI: 10.1111/omi. 12027

SUMMARY

Treponema denticola is an anaerobic spirochete whose abundance in the subgingival crevice correlates with the development and severity of periodontal disease. The ability of *T. denticola* to survive and thrive in the hostile environment of the periodontal pocket is due, at least in part, to its ability to bind factor H (FH), a negative regulator of the alternative complement pathway. The FH binding protein of *T. denticola* has been identified as FhbB and its atomic structure has been determined. The interaction of FH with *T. denticola* is unique in that FH bound to the cell surface is cleaved by the *T. denticola* protease, dentilisin. It has been postulated that FH cleavage by *T. denticola* leads to immune dysregulation in periodontal pockets. In this study, we conduct a comparative assessment of the sequence, properties, structure and ligand binding kinetics of the FhbB proteins of strains 33521 and 35405. The biological outcome of the interaction of these strains with FH could differ significantly as 33521 lacks dentilisin activity. The data presented here offer insight into our understanding of the interactions of *T. denticola* with the host and its potential to influence disease progression.

INTRODUCTION

Periodontal disease is among the most common infections of adults. In the USA alone, approximately 116 million adults have some form of periodontal disease (Beck, 1987; Darveau, 2010). Periodontitis begins with bleeding and inflammation of the gums (gingivitis) and can progress to gingival degradation, alveolar bone loss and endentulism (tooth loss). As disease develops there is a significant transition in the overall composition of the oral microflora with *Treponema denticola* becoming a dominant species (Socransky *et al.*, 1998; Ellen & Galimanas, 2005). *Treponema denticola* is a well-characterized anaerobic spirochete that has been clearly linked to periodontal disease severity (Loesche, 1988; Simonson *et al.*, 1988). Recent evidence suggests that expansion of the *T. denticola* population in the subgingival crevice leads to immune dysregulation and thereby creates conditions that exacerbate disease progression (McDowell *et al.*, 2011; Miller *et al.*, 2012).

The subgingiva are bathed in crevicular fluid, a serum and cell exudate rich in immune effectors including active complement (Schenkein & Genco, 1977; Boackle *et al.*, 1978; Boackle, 1991; Schenkein, 1991). Consistent with its ability to thrive in periodontal pockets, *T. denticola* strain 35405 is resistant to human serum concentrations as high as 25%

(McDowell *et al.*, 2011). The ability of *T. denticola* to resist serum-mediated killing is due to the binding of factor H (FH) (McDowell *et al.*, 2005), a negative regulator of the alternative complement pathway (Ruddy & Austen, 1969, 1971). FH is a 155-kDa glycoprotein that is composed of 20 imperfect repeat domains termed complement control protein (CCP) domains (Ferreira *et al.*, 2010). In the healthy host, FH prevents complement activation by: (i) serving as a cofactor for the factor I-mediated cleavage of C3b (a critical opsonin), (ii) blocking C3 convertase complex formation and (iii) accelerating decay of preformed C3 convertase complex (Zipfel *et al.*, 2002; Zipfel & Skerka, 2009). FH also contributes to regulation of complement activation by interacting with monomeric C-reactive protein (mCRP) (Jarva *et al.*, 1999). The FH-mCRP complex enhances inactivation of C3b (Mihlan *et al.*, 2009). In addition, FH-mCRP plays an important role in regulating inflammatory responses by inhibiting the production of proinflammatory cytokines (Mihlan *et al.*, 2009). Several pathogens exploit the negative regulatory activity of FH. The FH bound to the surface of pathogens functions to downregulate complement activation locally at the cell surface (reviewed in Zipfel *et al.*, 2007).

FH binding proteins produced by different bacterial species represent a diverse group with little or no sequence or structural homology. The FH binding protein of *T. denticola* is a 11.4-kDa protein designated as FhbB (McDowell *et al.*, 2005, 2007). The atomic structure of FhbB has been solved at 1.7 Å resolution (Miller *et al.*, 2011, 2012). The FhbB structure is unique, consisting of an $\alpha\alpha\beta\alpha\beta$ fold with well-defined negatively and positively charged faces. Mutagenesis studies demonstrate that FH interacts with the negatively charged face of FhbB (Miller *et al.*, 2012). A unique aspect of the *T. denticola*–FH interaction is that bound FH is cleaved by dentilisin (McDowell *et al.*, 2009). Dentilisin is a multi-subunit protease that is thought to mediate several aspects of *T. denticola* pathogenesis (Fenno & McBride, 1998; Fenno, 2012). It has been hypothesized that FhbB–dentilisin-mediated cleavage of FH may deplete local FH concentrations resulting in immune dysregulation, thereby creating conditions that favor the progression of periodontal disease (Miller *et al.*, 2012).

To date, studies that have sought to define the molecular basis of the interaction of FH with FhbB have been focused exclusively on the *T. denticola*

type strain, 35405. Earlier sequence analyses of *fhbB* from strains 35405, GM1 and 33520 suggested that FhbB is highly conserved (McDowell *et al.*, 2007). In this study we characterize a divergent FhbB ortholog derived from *T. denticola* 33521 (FhbB₃₃₅₂₁) and use this natural FhbB variant to further assess the molecular basis of the FH–FhbB interaction. The analyses presented here provide insight as to how different strains of *T. denticola* may influence the development and progression of periodontal disease.

METHODS

Bacterial strains, DNA sequencing and generation of recombinant (r-) proteins

Treponema denticola strains 35405 and 33521 were grown in new oral spirochete media under anaerobic conditions (McDowell *et al.*, 2011). Cells were harvested by centrifugation and genomic DNA was isolated as previously described (McDowell *et al.*, 2007). Polymerase chain reaction analysis was performed using standard conditions with primers designed to amplify the full-length *fhbB* gene including upstream and downstream flanking sequences. All primer sequences are provided in Table 1. The resulting amplicons were TA cloned and sequenced on a fee-for-service basis (Genewiz, South Plainfield, NJ). To allow for production of r-FhbB, additional primers were designed to amplify the coding sequence (minus the sequence encoding the 23-amino-acid leader peptide). Sequences that allow for ligase-independent cloning (indicated by underlining in Table 1) with the pET32 Ek/LIC or pET46 Ek/LIC vectors (Novagen, Darmstadt, Germany) were included in each primer. Proteins expressed using the pET32 Ek/LIC vector possess a 17-kDa N-terminal fusion containing 6x-His and S-tags. Proteins produced using pET46 Ek/LIC harbor a 3-kDa N-terminal fusion that contains a 6x-His tag. All cloning procedures were conducted as previously described (Miller *et al.*, 2012). Recombinant FH proteins consisting of different CCP domains were produced with N-terminal 6x-His tags as previously described (Miller *et al.*, 2012). Specifically, r-proteins spanning CCP1–4, CCP5–7, CCP6–8, CCP8–13, CCP14–18 and CCP19–20 were generated. R-FhbA, an FH binding protein derived from *Borrelia hermsii*, was generated in an earlier study (Hovis *et al.*, 2008) and used as a control.

Table 1 Oligonucleotide primers (5'–3') used in this study

TDE0107Up	TTTATTCCACCATTCCATACATC
TDE0109Rev	CGATATTCATGACGTTTACTAC
FhbB33521LIC (+)	<u>GACGACGACAAGATT</u> CGTTTTAAATGAATACTGCAC
FhbB33521LIC (–)	<u>GAGGAGAAGCCCGTT</u> ACTTTTTCTTGGGTACAAAG
CCP1LIC(+)	<u>GACGACGACAAGGAAG</u> ATTGCAATGAACCTCCTCC
CCP4LIC(–)	<u>GAGGAGAAGCCCGTT</u> CATGATTTTTCTTCACATGAAGGCAACG
CCP5LIC(+)	<u>GACGACGACAAGAAAT</u> CATGTGATAATCCTTATATTC
CCP7LIC(–)	<u>GAGGAGAAGCCCGTT</u> CAGACACGGATGCATCTGGGAGTAG
CCP8LIC(+)	<u>GACGACGACAAGAAAAA</u> ACATGTTCCAAATCAAGTATAG
CCP13LIC(–)	<u>GAGGAGAAGCCCGTT</u> CATGCCATTGAGCAGTTCACTTC
CCP14LIC(+)	<u>GACGACGACAAGAAACA</u> ATTATGCCACCTCCACCTC
CCP18LIC(–)	<u>GAGGAGAAGCCCGTT</u> CAAGAATCTTTCATTGAGGTGGTTC
CCP19LIC(+)	<u>GACGACGACAAGATCAA</u> AGATTCTACAGGAAAATGTG
CCP20LIC(–)	<u>GAGGAGAAGCCCGTT</u> CTATCTTTTGCACAAGTTGGATAC
521E43K(+)	GGTCTTAAAAATGATGTAAAAGATAA
521E43K(–)	TTATCTTTTACATCATTTTTAAGACC
521E43D(+)	GGTCTTGACAATGATGTAAAAGATAA
521E43D(–)	TTATCTTTTACATCATTGTCAAGACC
521E43G(+)	GGTCTTGGAATGATGTAAAAGATAA
521E43G(–)	TTATCTTTTACATCATTTCAGACC
521D45K(+)	GGTCTTGAAAATAAAGTAAAAGATAA
521D45K(–)	TTATCTTTTACTTTATTTTCAAGACC
521D45E(+)	GGTCTTGAAAATGACGTAAAAGATAA
521D45E(–)	TTATCTTTTACGTCATTTTCAAGACC
521D45G(+)	GGTCTTGAAAATGGTGTAAAAGATAA
521D45G(–)	TTATCTTTTACACCATTTTCAAGACC
521D45A(+)	GGTCTTGAAAATGCTGTAAAAGATAATCCAATGACTGC
521D45A(–)	GCAGTCATTGGATTATCTTTTACAGCATTTTCAAGACC
521D48A(+)	GGTCTTGAAAATGATGTAAAAGCTAATCCAATGACTGC
521D48A(–)	GCAGTCATTGGATTAGCTTTTACATCATTTTCAAGACC
521E58A(+)	CAAAATGTGAAAGCAGGGCTTGATCTTGC
521E58A(–)	GCAAGATCAAGCCCTGCTTTCACATTTTG
521D61A(+)	GAAGGGCTTGCTCTTGCTAATGTGC
521D61A(–)	CGACATTAGCAAGAGCAAGCCCTTC

The portions of each primer that were included to allow for annealing with the pET LIC vectors are indicated by underlining.

Generation of antisera

Anti-FhbB₃₅₄₀₅ and anti-FhbB₃₃₅₂₁ antisera were generated in C3H-HeJ mice (three per antigen) as previously described (McDowell *et al.*, 2011). In brief, 20 µg r-protein in alum (with two boosts) was administered to each mouse ($n = 3$) (Earnhart *et al.*, 2007). Anti-FhbB₃₅₄₀₅ and anti-FhbB₃₃₅₂₁ antisera were also generated in female Sprague-Dawley rats (two per antigen). The rats were anesthetized using a cocktail containing ketamine/xylazine/acepromazine and then injected intraperitoneally with 40 µg r-protein diluted in sterile phosphate-buffered saline (PBS) and mixed 1 : 1 with complete Freund's adjuvant (total volume 0.5 ml per rat) (Sigma–Aldrich, St Louis, MO). Three weeks and 5 weeks after the primary immunization, animals were boosted with 40 µg of the same antigen diluted in PBS

and mixed with incomplete Freund's adjuvant (Sigma–Aldrich). Two weeks following the final boost, animals were exsanguinated by cardiac puncture under anesthesia and serum was harvested by centrifugation.

All animal experiments were conducted following the *Guide for the Care and Use of Laboratory Animals* (eighth edition) and in accordance with protocols peer-reviewed and approved by Virginia Commonwealth University and the University of Connecticut Health Center Institutional Animal Care and Use Committees.

Computer-assisted structural modeling

A structural model of FhbB₃₃₅₂₁ was created using the known structure of FhbB₃₅₄₀₅ (pdb code 3R15) (Miller

et al., 2011, 2012) and MODELER 9v1 (Sali, 1995; Sali *et al.*, 1995). Briefly, CLUSTALW2 (Larkin *et al.*, 2007) was used to align the FhbB₃₅₄₀₅ and FhbB₃₃₅₂₁ sequences (residues 24–101). Models were generated, compared with the FhbB₃₅₄₀₅ structure and evaluated by MOLPROBITY to assess all-atom contacts and geometry (version 3.15) (Davis *et al.*, 2007).

FH affinity ligand binding immunoblots, Western blots and ELISA

Factor H affinity ligand binding immunoblot assays were performed as previously described (Miller *et al.*, 2012). In brief, r-FhbB proteins were fractionated by sodium dodecyl sulfate–polyacrylamide gel electrophoresis (SDS–PAGE) in 15% Criterion gels (Bio-Rad, Hercules, CA) and transferred to Immobilon-P membranes by electroblotting. The membranes were overlaid with purified human FH (10 µg ml⁻¹; Complement Technologies, Tyler, TX) or the CCP constructs. Binding was detected using goat anti-FH antiserum (1 : 1000) (Complement Tech.) with rabbit anti-goat immunoglobulin G (IgG) serving as the secondary antiserum (1 : 20,000). Signal was detected by chemiluminescence using the SuperSignal ECL substrate (Thermo Scientific, Rockford, IL).

Western blot analyses were performed using standard, previously described methods (McDowell *et al.*, 2011). Mouse anti-FhbB and rat anti-FhbB antisera were used at dilutions of 1 : 1000 and 1 : 5000, respectively. Secondary antibodies were used at a dilution of 1 : 40,000. Signal was detected by chemiluminescence using the SuperSignal ECL substrate (Thermo Scientific). Enzyme-linked immunosorbent assays (ELISA) were conducted as previously described (Miller *et al.*, 2012). In brief, r-FhbB proteins, r-FhbA (positive control) and bovine serum albumin (negative control) were immobilized in the wells of 96-well microtiter plates (in triplicate; 1 µg per well in 100 mM NaHCO₃, pH 9.6, overnight; 4°C). Non-specific binding was blocked with PBS with 0.2% Tween-20 (PBST) with 5% non-fat dry milk (PBSTM) (1 h, at room temperature). CCP constructs and full-length FH (10 µg ml⁻¹ in PBST) were added to the wells (in triplicate) for 1 h followed by three washes with PBST. Goat anti-human FH (1 : 800 in PBSTM; Complement Tech.) was added to each well (1 h, room temperature). The plates were washed (three times) and then rabbit anti-goat IgG (1 : 20,000

dilution in PBSTM; Calbiochem, Darmstadt, Germany) was added (1 h). The plates were again washed (three times) and then antibody binding was detected using 2,2'-azino-bis(3-ethylbenzothiazoline-6-sulphonic acid) at 405 nm.

Indirect-immunofluorescence assays

Indirect immunofluorescence assays (IFAs) were conducted as previously described (McDowell *et al.*, 2005). In brief, duplicate slides were generated for each strain and air dried. One set of slides was treated with acetone to permeabilize the cells (fixed) while the second set was not treated (unfixed). Mouse anti-FhbB₃₅₄₀₅, mouse anti-FhbB₃₃₅₂₁ or goat anti-FlaA antiserum (1 : 500 dilution) was then added to the slides and antibody binding was detected using Alexa 568-conjugated goat anti-mouse IgG antibody or Alexa 488-conjugated goat anti-rabbit IgG antibody (1 : 1000 in PBST, 3% bovine serum albumin). Cells were also visualized by dark-field microscopy. Images were captured with a DP71 camera (Olympus, Center Valley, PA).

Triton X-114 extraction and phase partitioning

Cells were recovered by centrifugation (0.5 OD₆₀₀), extracted with 1% Triton X-114 and phase-partitioned (three times) as previously described (Roberts *et al.*, 2000). The aqueous phase was concentrated five-fold with Amicon Ultra 3,000 Da cut-off filters (Millipore, Billerica, MA). The detergent phase was concentrated by precipitation with five volumes of ice-cold acetone followed by centrifugation (15,000 g, 30 min, 4°C). The samples were solubilized with SDS–PAGE loading buffer, analyzed by SDS–PAGE, transferred to Immobilon-P membranes by electroblotting and screened with rat anti-FhbB₃₅₄₀₅, rat anti-FhbB₃₃₅₂₁ and rabbit anti-FlaA antisera using standard procedures. Antibody binding was detected using the appropriate secondary antibody and chemiluminescence.

Surface plasmon resonance

FhbB-FH binding kinetic analyses were performed using a Biacore T100 and the data evaluated using BIAEVALUATION V 1.1 (Biacore, Uppsala, Sweden) as previously detailed (Miller *et al.*, 2012). In brief, r-FhbB proteins (ligand) were immobilized to an nitrilotriacetic

acid chip (GE Healthcare, Buckinghamshire, United Kingdom) via their N-terminal His-tag and increasing concentrations of purified FH (analyte; Complement Tech) were provided in the fluid phase. The kinetics data were fit to a Langmuir 1 : 1 binding model and averaged from at least two replicate experiments.

Site-directed mutagenesis

Site-directed mutagenesis was performed as previously described using a mutagenic PCR-based approach with primers that allow for ligase-independent cloning into the pET32 Ek/LIC and pET46 Ek/LIC vectors (Miller *et al.*, 2012). All methods associated with the generation, production and purification of r-proteins were as previously described (Miller *et al.*, 2012). FH binding to each r-protein was assessed using assays detailed above.

Measurement of dentilisin activity

The dentilisin activity of each strain was measured by monitoring hydrolysis of succinyl-L-alanyl-L-alanyl-L-prolyl-L-phenylalanyne-*p*-nitroanilide (SAAPFNA; Sigma–Aldrich) (Uitto *et al.*, 1988; McDowell *et al.*, 2011). In brief, aliquots of fresh, mid-log phase cultures were placed in buffer A (100 mM NaCl, 1 mM CaCl₂, 50 mM Tris–HCl pH 8.0) and transferred to the wells of a 96-well plate. SAAPFNA was added (1 mM in buffer A), the plates were incubated (30 min, 37°C) and SAAPFNA hydrolysis was measured by monitoring absorbance at 405 nm. The dentilisin-deficient strain, 35405-CCE (Bian *et al.*, 2005), served as a control.

FH proteolysis assays

The ability of each strain to degrade purified FH was assessed as previously described (McDowell *et al.*, 2011). In brief, 0.05 OD₆₀₀ of freshly harvested mid-log phase *T. denticola* cells were incubated in PBS with purified FH (80 µg ml⁻¹, 1 h, 37°C). The samples were then solubilized, fractionated by SDS–PAGE, immunoblotted and screened for FH proteolysis using anti-human FH antiserum (as described above).

Serum sensitivity assay

The sensitivity of strains 35405 and 33521 to killing by human serum was determined as previously

described (McDowell *et al.*, 2011). Cells from mid-log phase cultures were incubated with 25% complement-preserved normal human serum (NHS; Innovative Research, London, UK) in new oral spirochete media (3 h, 37°C, anaerobic conditions). As a control the strains were also incubated with 25% heat-inactivated NHS (HIS) (56°C, 30 min). In all cases the new oral spirochete media and human serum were equilibrated to anaerobic conditions before use. The percentage of morphologically intact cells (intact cells/total number of intact and morphologically disrupted cells) was determined by cell counting under dark field microscopy (three fields; 400 × magnification). Three biological replicates were performed and the results averaged.

RESULTS

Determination and analysis of the *T. denticola* strain 33521 *fhbB* sequence

Before this study, *fhbB* sequences from three different strains (35405, 33520 and GM-1) have been reported in the literature (McDowell *et al.*, 2007). These sequences were found to be highly conserved with only a single nucleotide difference. Determination and analysis of the *fhbB*₃₃₅₂₁ sequence revealed 60.8 and 73.4% amino acid identity and similarity, respectively, with FhbB₃₅₄₀₅. An alignment of the sequences highlighting structural domains or motifs is presented in Fig. 1. Sequence differences are concentrated within the region analogous to the negatively charged α1α2 domain that forms the FH binding interface (Miller *et al.*, 2012). The DNA sequences that flank the *fhbB* genes of strains 35405 and 33521, including the *fhbB* promoter, are highly conserved but harbor some

	Leader Peptide	$\alpha 1$	$\alpha 2$	
35405	MKNKRIFTVLFLAVSALLFTSCTFRMNTAQKAHYEKFINALENELKTRHIPAGAVIDM			
33521VL.....S..A.....A..SG...DV.DNPM.T.QN.KEG			
	$\alpha 2$	$\beta 1$	$\alpha 3$	$\beta 2$
35405	LAETINTEALALDYQIVDKKPGTSIAQGTAKAAALRRKRFIPKKIK			
33521	.DLA.VG.A..NFK.....A..E..K.....E.....V.....			

Figure 1 FhbB sequence alignment. The DNA sequences of *fhbB*₃₅₄₀₅ and *fhbB*₃₃₅₂₁ were determined as described in the text and translated. The amino acid sequences were aligned using CLUSTALW. The leader peptide and structural domains previously determined through X-ray crystallography for the FhbB₃₅₄₀₅ protein are indicated above the sequences. The Factor H (FH) binding interface of FhbB₃₅₄₀₅ extends from alpha helix 1 (α1) through alpha helix 2 (α2). Identical residues are indicated by periods and gaps by (–).

polymorphisms. *fhbB*₃₃₅₂₁ possesses a 48-bp deletion downstream of the stop codon within the putative rho-independent terminator. It remains to be determined if this deletion influences the transcriptional expression of *fhbB* in strain 33521 (data not shown).

FhbB₃₅₄₀₅ and FhbB₃₃₅₂₁ variants are antigenically distinct

To determine if FhbB₃₅₄₀₅ and FhbB₃₃₅₂₁ are antigenically distinct, antisera to both proteins were individually generated in rats and used to screen immunoblots of r-FhbB₃₅₄₀₅, r-FhbB₃₃₅₂₁ and r-FhbA. FhbA is a FH binding protein derived from the relapsing fever spirochete, *Borrelia hermsii* (Hovis *et al.*, 2004), that served as a negative control (Fig. 2). The antisera proved to be variant specific with no cross-reactivity. Collectively, the data indicate that antibody responses are directed at variable amino acids within the putative FH interaction domain.

FhbB is an amphipathic surface-exposed lipoprotein

Strains 35405 and 33521 were subjected to Triton X-114 extraction and phase partitioning. Immunoblot analysis of the resulting fractions using anti-FhbB₃₅₄₀₅, anti-FhbB₃₃₅₂₁ and anti-FlaA antiserum (control) revealed that FhbB partitions predominantly

with the detergent phase indicating amphipathic properties consistent with a lipoprotein (Fig. 3). As expected, FlaA (a component of the inner membrane-anchored periplasmic flagella) partitioned with the insoluble phase.

FhbB surface localization was also assessed by IFA. Labeling of non-permeabilized cells with anti-FhbB antibody was observed for strains 35405 and 33521 but not 35405Δ*fhbB* (Fig. 4). Cell integrity was verified by screening slides with anti-FlaA antiserum. FlaA is a major component of the inner membrane anchored-periplasmic flagella. Only acetone permeabilized cells were labeled with the anti-FlaA antibody. Collectively these analyses demonstrate that FhbB is a surface-exposed outer membrane protein with properties consistent with a lipoprotein.

FhbB₃₅₄₀₅ and FhbB₃₃₅₂₁ are similar in structure and surface charge distribution

The FhbB₃₃₅₂₁ sequence was threaded onto the previously determined high-resolution (1.7 Å) atomic structure of FhbB₃₅₄₀₅ (Miller *et al.*, 2011, 2012). Five models each with an average root mean-squared deviation of 0.17 Å were obtained. The models were then evaluated using MolPROBITY (Chen *et al.*, 2010). The model depicted in Fig. 5 for FhbB₃₃₅₂₁ had the fewest all-atom clashes with 98% of residues in favored Ramachandran phi-psi angles. These

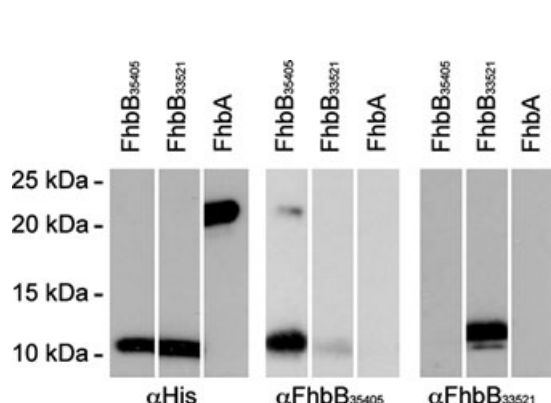


Figure 2 FhbB variants are antigenically distinct. Recombinant proteins (indicated above each lane) were produced as 6X-His-tagged fusions, purified, subjected to sodium dodecyl sulfate–polyacrylamide gel electrophoresis and transferred to membranes. The membranes were screened with antiserum as indicated below each panel. Molecular weights are indicated to the left. All methods are detailed in the text.

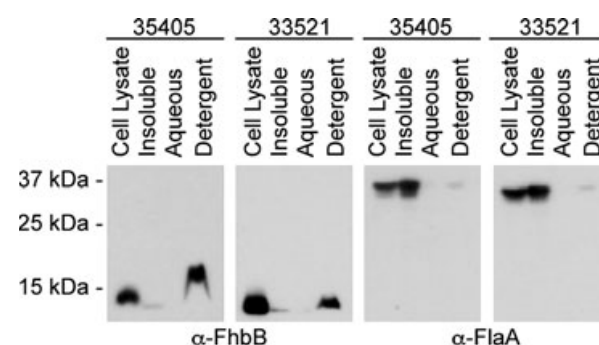


Figure 3 Triton X-114 extraction and phase partitioning of *Treponema denticola* demonstrate that FhbB is amphipathic. The *T. denticola* strains 35405 and 33521 were cultivated, harvested, washed, extracted with Triton X114 and phase partitioned as detailed in the text. The resulting fractions (as indicated above each lane) were assessed by sodium dodecyl sulfate–polyacrylamide gel electrophoresis, transferred to polyvinylidene fluoride membranes and screened with anti-FhbB antisera or anti-FlaA antisera. Molecular weight standards are indicated to the left.

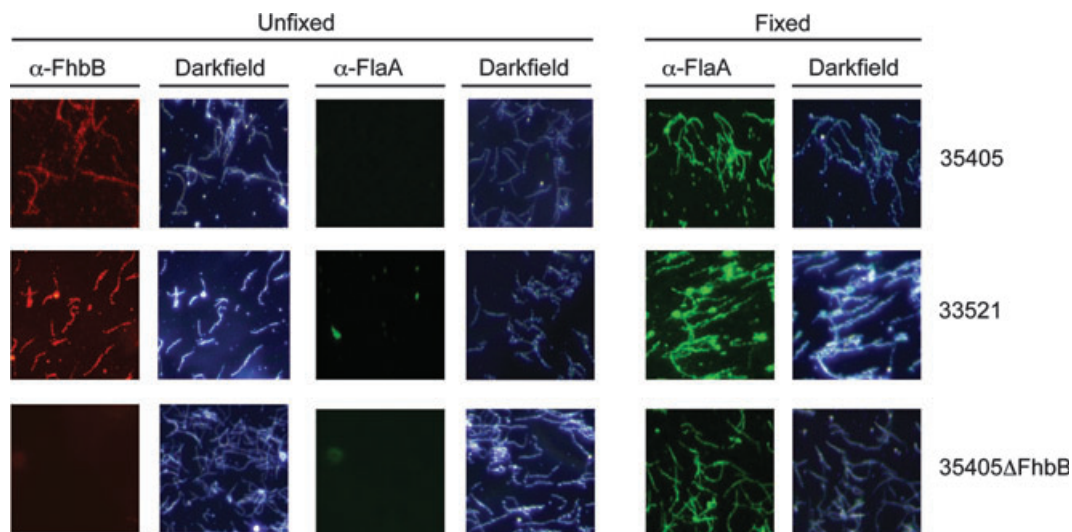


Figure 4 FhbB is presented on the *Treponema denticola* cell surface. Immunofluorescence assays were performed as detailed in the text. Intact (unfixed) or acetone permeabilized (fixed) *T. denticola* 35405, 33521 and 35405ΔFhbB cells (as indicated to the right of each row of images) were screened with anti-FhbB (α-FhbB) and anti-FlaA (α-FlaA) antiserum. Antibody binding was detected using fluorescently conjugated antibodies. Cells within each field of view were also visualized by dark-field microscopy.

analyses indicate a strong fit for the deduced structural model for FhbB₃₃₅₂₁ and suggest that in spite of significant sequence diversity, the overall structures of FhbB₃₃₅₂₁ and FhbB₃₅₄₀₅ are highly similar. The surface charge distribution for each protein was also compared. A stronger and more widely dispersed region of negative charge is predicted at the FH binding interface of FhbB₃₃₅₂₁.

Identification of the FhbB interaction site on FH

As noted above, sequence differences between FhbB₃₃₅₂₁ and FhbB₃₅₄₀₅ are concentrated within the FH binding interface. These differences could result in different molecular contact points with FH. FhbB₃₅₄₀₅ interacts with CCP7 of FH (McDowell *et al.*, 2012; Miller *et al.*, 2012). To determine if FhbB₃₃₅₂₁ interacts with the same FH domains as FhbB₃₅₄₀₅, ELISA-based binding analyses were conducted using full-length FH and r-constructs consisting of CCP1–4, CCP5–7, CCP6–8, CCP8–13, CCP14–18 and CCP19–20 (Fig. 6). FhbB₃₃₅₂₁ bound CCP5–7, CCP6–8 and full-length FH but not to other CCPs, localizing the binding site within CCPs 6 and 7. Bovine serum albumin served as a negative control and as expected, it did not bind to FH or to any of the CCP constructs. The binding results obtained through ELISA were subsequently confirmed using

affinity ligand binding immunoblot assays (data not shown). The integrity of the CCP fragments used in these binding assays was confirmed by SDS-PAGE and the ability of anti-FH antibody to recognize all of the CCP constructs was demonstrated by immunoblot analyses (data not shown). In addition, the biological competence of the r-CCP1–4 fragment to serve as a co-factor in the factor I-mediated cleavage of C3b was verified using a C3b cleavage assay (data not shown).

FH binding kinetics

To compare the binding kinetics of FH with r-FhbB₃₃₅₂₁ and FhbB₃₅₄₀₅, surface plasmon resonance analyses were performed. The FhbB proteins were coupled to nitrilotriacetic acid chips and purified FH was provided in the fluid phase. The K_D for the r-FhbB₃₃₅₂₁–FH interaction was determined to be $9.01 \pm 0.09 \times 10^{-7}$ M with a k_a of $3.41 \pm 0.72 \times 10^4$ M⁻¹ s⁻¹ and a k_d of 0.0307 ± 0.0062 s⁻¹ (Fig. 7). In contrast, the K_D for the r-FhbB₃₅₄₀₅–FH interaction was determined to be $1.51 \pm 0.02 \times 10^{-6}$ M with a k_a of $7.56 \pm 0.26 \times 10^4$ M⁻¹ s⁻¹ and k_d of 0.11 ± 0.01 s⁻¹ (Miller *et al.*, 2012). Hence, the FhbB₃₃₅₂₁–FH interaction is characterized by slower on and off rates and a stronger binding affinity (relative to the FhbB₃₅₄₀₅–FH interaction).

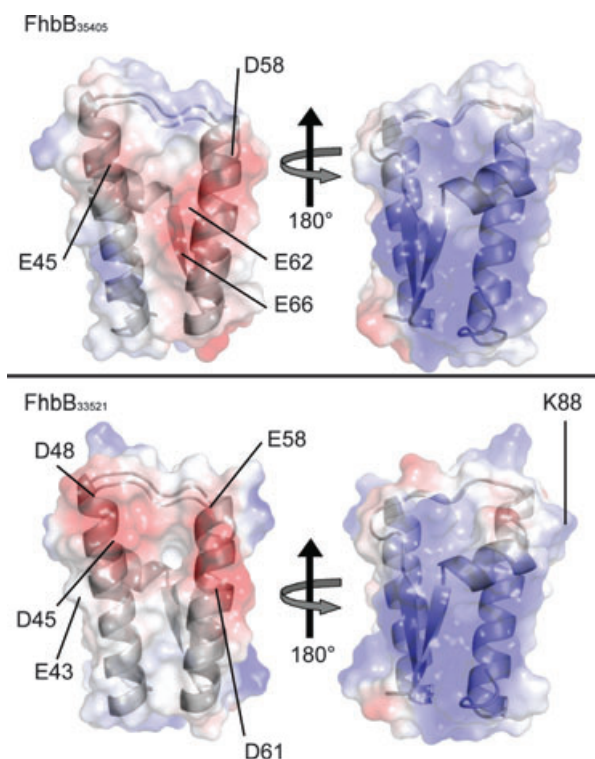


Figure 5 Structural modeling of FhbB. The determined and predicted structures for FhbB₃₅₄₀₅ (top panel, PDB 3R15) and FhbB₃₃₅₂₁ (bottom panel) are shown as ribbon diagrams with surface electrostatic charges (red, negative charge; blue, positive charge). The left panel presents a head on view of the Factor H binding interface. The images in the right panels are rotated 180° around the y-axis. The location of residues that were targeted for site-directed mutagenesis or that are discussed in the text are indicated.

Site-directed mutagenesis of FhbB: identification of residues involved in the FhbB–FH interaction

Earlier site-directed mutagenesis analyses of FhbB₃₅₄₀₅ and FH identified residues in both proteins that are important molecular determinants in the binding interaction (McDowell *et al.*, 2005, 2009; Miller *et al.*, 2012). To identify residues that play a role in the FH–FhbB₃₃₅₂₁ interaction, site-directed mutagenesis analyses were conducted. The following individual substitutions were introduced into FhbB₃₃₅₂₁: E43K, E43D, E43G, D45K, D45E, D45G, D45A, D48A, D58A and D61A. The spatial location of each residue in the FhbB structure is indicated in Fig. 5. R-proteins harboring these individual substitutions were generated, purified and tested for FH binding using affinity ligand binding immunoblot assays (Fig. 8). Residue E43 was targeted because in FhbB₃₅₄₀₅ residues E43

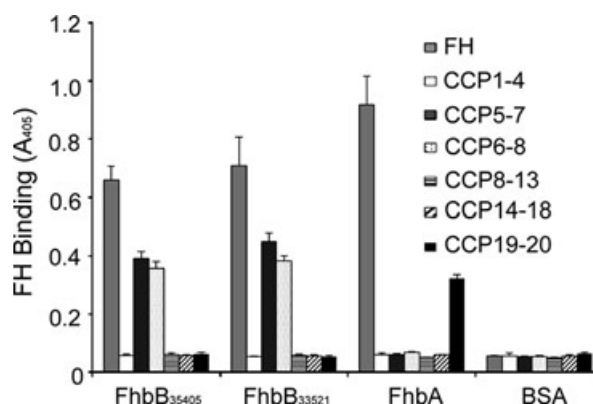


Figure 6 Divergent FhbB variants interact with CCP6-7 of Factor H (FH). R-FhbB₃₅₄₀₅, FhbB₃₃₅₂₁, FhbA and bovine serum albumin (BSA) were immobilized in the wells of enzyme-linked immunosorbent assay plates and screened with r-proteins spanning different complement control protein (CCP) domains of FH (indicated in the insert). FhbA, which has been demonstrated to bind to CCP19–20, served as a positive control. BSA, which does not bind FH, served as a negative control. Binding of the CCP constructs was measured using an enzyme-linked immunosorbent assay format as detailed in the text.

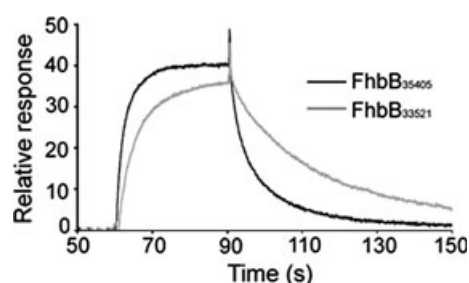


Figure 7 Analysis of the kinetics of the interaction of Factor H (FH) with FhbB₃₅₄₀₅ and FhbB₃₃₅₂₁. Binding kinetics were assessed using surface plasmon resonance. R-FhbB proteins were immobilized on a nitrilotriacetic acid chip and various concentrations of FH were added in the fluid phase. The binding curve obtained using FH at a concentration of 2.5 μ M is presented.

and K88 form a salt-bridge between α 1 and α 3. These residues are conserved suggesting that the E43–K88 salt bridge is an important structural component in FH binding (McDowell *et al.*, 2007; Miller *et al.*, 2012). However, E43D, E43K and E43G substitutions had little or no effect on FH binding demonstrating that the E43–K88 salt bridge is not required for FH binding. Residue D48 was targeted because it is a negatively charged residue located within the predicted FH binding domain of FhbB. Substitution of D48 with A had no effect on FH binding. In an earlier

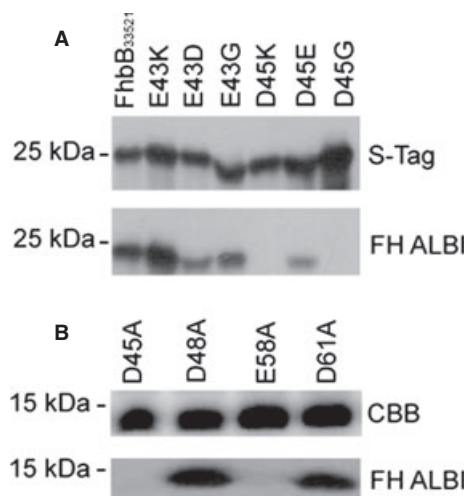


Figure 8 Identification of FhbB residues required for Factor H (FH) binding. Site-directed amino acid substitutions were introduced into FhbB using a mutagenic polymerase chain reaction approach. Recombinant proteins were generated, purified, fractionated by sodium dodecyl sulfate–polyacrylamide gel electrophoresis and transferred to membranes. Note that the substitution mutants were generated using two different expression vectors and hence the results are presented in two panels. The proteins tested in (A) were generated in pET32 Ek/LIC whereas those in (B) were generated using pET46 Ek/LIC vector. To verify protein loading, the top blot in (A) was screened with S-Protein as previously described (McDowell *et al.*, 2002). In (B) the protein loading was assessed by staining of a duplicate gel with Coomassie brilliant blue G250 (CBB). The membranes were incubated with purified FH and binding was detected with FH-specific antisera. As a loading controls, identical blots were screened with horseradish peroxidase-conjugated S-protein to detect the N-terminal expression tag.

study, other nearby negatively charged residues (E45, D58 and E62) were demonstrated to influence the FhbB₃₅₄₀₅–FH interaction (Miller *et al.*, 2012). In FhbB₃₃₅₂₁, the identity of the residues at positions 45 (D) and 58 (E) differs from strain 35405 (E and D, respectively) but negative charge is retained. Substitution of these residues with Ala abolished FH binding, confirming the previously reported critical requirement to maintain negative charge at these positions (McDowell *et al.*, 2007; Miller *et al.*, 2012). The importance of D/E45 and D/E58 in binding is consistent with their spatial placement in FhbB. These residues sit on the surface accessible faces of $\alpha 1$ and $\alpha 2$. In FhbB₃₅₄₀₅, E62 was identified as a critical residue for FH binding (Miller *et al.*, 2012). When substituted with Ala, FH binding was completely lost. Interestingly, while FhbB₃₃₅₂₁ has a Leu at position 62, position 61 is an Asp residue. We speculated that

negative charge at residue 61 compensates for the absence of negative charge at residue 62. However, a D61A substitution mutant retained FH binding, indicating subtle differences in the residues required for FH binding between these FhbB orthologs. The data presented here provide additional insight into the molecular basis of the FhbB–FH interaction and support the conclusion that the $\alpha 1\alpha 2$ face of FhbB serves as the interaction platform for FH.

33521 lacks dentilisin activity and FH cleavage

There are conflicting reports regarding the dentilisin phenotype of strain 33521 (Heuner *et al.*, 2001; Wyss *et al.*, 2004; Goetting-Minesky *et al.*, 2012). Wyss *et al.* and Goetting-Minesky *et al.* determined strain 33521 to be negative for dentilisin activity while Heuner *et al.* reported it to be dentilisin positive. To independently assess dentilisin activity, SAAPFNA assays were conducted (Fig. 9). Strain 35405 (dentilisin positive) and 35405-CCE (a dentilisin-deficient strain) (Bian *et al.*, 2005) served as positive and negative controls, respectively. An absorbance change of 0.71 ± 0.02 was measured for 35405-CCE, representing a baseline for this assay. Strain 35405, which has strong dentilisin activity, resulted in an absorbance change of 3.51 ± 0.07 . Strain 33521 had an absorbance change below baseline, 0.56 ± 0.02 , indicating that 33521 does not have dentilisin activity. Dentilisin has been demonstrated to cleave FH bound to the *T. denticola* surface (McDowell *et al.*, 2009). Hence we also used FH cleavage as a readout of potential dentilisin activity (Fig. 9). While the positive control strain (35405) completely cleaved the input FH, FH cleavage was not observed with 33521 or 35405-CCE. Collectively, these results demonstrate that strain 33521 is incapable of FH cleavage.

Strain 33521 is resistant to human serum

Incubation of 35405, 33521 and 35405 Δ fhbB with 25% NHS resulted in 12, 8 and 49% killing, respectively (Fig. 10). No significant killing was observed with HIS. The serum sensitivity levels observed here for strains 35405 and 35405 Δ fhbB are consistent with an earlier report that demonstrated the importance of FhbB in evasion of complement-dependent serum-mediated killing (McDowell *et al.*, 2011). The slightly better percentage survival rate of the 33521 strain,

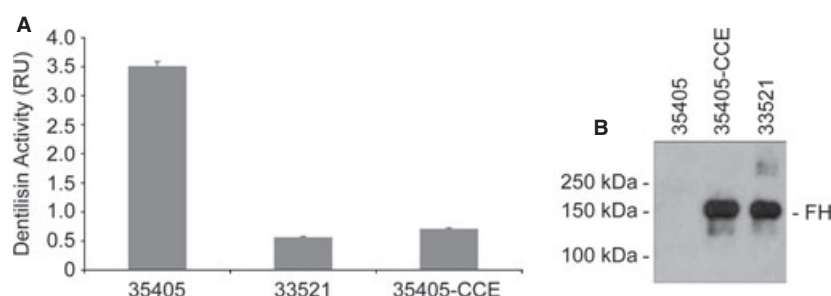


Figure 9 Strain 33521 lacks dentilisin activity and fails to degrade bound Factor H (FH). (A) Dentilisin activity of strain 33521 was analyzed by measuring SAAPFNA cleavage. Strain 35405 and 35405-CCE (a dentilisin-deficient strain) served as positive and negative controls, respectively. All methods were as detailed in the text. (B) The ability of each strain to cleave FH was assessed through immunoblot analysis of FH that had been incubated with whole cells (as indicated). FH breakdown was monitored using anti-human FH antiserum.

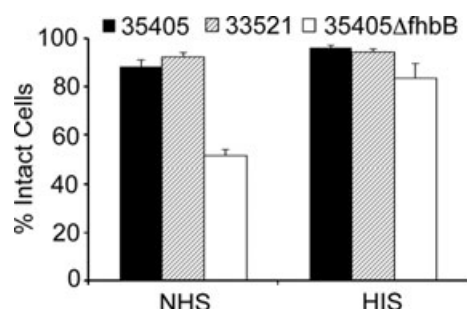


Figure 10 Analysis of the sensitivity of *Treponema denticola* strains to human serum. Strains 35405 (black), 33521 (dashed lines), and 35405ΔfhhB (white) were incubated in 25% complement-preserved normal human serum (NHS) or in heat-inactivated NHS (HIS) for 3 h. The percentage of intact cells was determined through dark-field microscopy. The data presented are an average of three individual experiments.

relative to a dentilisin-positive strain (35405) suggests that dentilisin may slightly decrease complement resistance, presumably as a consequence of FH cleavage.

DISCUSSION

Complement evasion mediated by the binding of FH is an important virulence mechanism for a diverse range of pathogens (Zipfel *et al.*, 2008) including the periopathogen, *T. denticola* (McDowell *et al.*, 2012). While more than 70 species of treponemes have been identified in the subgingival crevice (Paster *et al.*, 2006), *T. denticola* is the only species shown to bind FH (McDowell *et al.*, 2005). In addition, it is the only bacterial species that has been demonstrated to cleave FH bound to its surface (McDowell *et al.*, 2009). The cleavage of FH may lead to its local

depletion, resulting in a cascade of events that favors the growth of the periopathogen consortium and the progression of periodontal disease (McDowell *et al.*, 2012; Miller *et al.*, 2012). Understanding how FH interacts with different *T. denticola* strains will enhance our understanding of the role of FH binding and the epidemiology of periodontal disease.

In this study we have assessed the properties of a unique variant of FhbB carried by the *T. denticola* strain 33521. To date, analyses of the FhbB–FH interaction have focused exclusively on strain 35405 (McDowell *et al.*, 2005, 2007, 2009, 2011, 2012; Miller *et al.*, 2011, 2012). The *fhhB* gene was PCR amplified from strain 33521 using primers designed based on the strain 35405 genome sequence that targets flanking regions of *fhhB*. Sequence analyses revealed that *fhhB*₃₃₅₂₁ differs significantly from previously reported *fhhB* sequences (McDowell *et al.*, 2007) sharing only 60.8% amino acid identity and 73.4% similarity with FhbB₃₅₄₀₅. Sequence differences were concentrated within the FH binding interface domain. Within this domain FhbB₃₃₅₂₁ displays 53 and 64% amino acid identity and similarity, respectively, with FhbB₃₅₄₀₅. In contrast, the identity and similarity values of the opposite face of the protein are 74 and 90%, respectively. Although the FH binding interface is the most variable domain of the protein, FhbB₃₃₅₂₁ retains FH binding ability. Although considerable sequence differences exist between these FhbB orthologs, molecular modeling analyses predict that FhbB₃₃₅₂₁ and FhbB₃₅₄₀₅ are of similar structure.

It has been postulated that the interaction between bacterially produced FH binding proteins and FH is dependent on the presentation of the proper electrostatic environment and not on a strictly defined

primary sequence (Miller *et al.*, 2012). The divergence within the FH binding interface of these FhbB orthologs supports this suggestion. The electrostatic surface charge maps of FhbB₃₃₅₂₁ and FhbB₃₅₄₀₅ are similar with well-defined positively charged ($\beta 1\alpha 3\beta 2$) and negatively charged ($\alpha 1\alpha 2$) faces. The stronger and more widely dispersed negative-surface charge region of the $\alpha 1\alpha 2$ face of FhbB₃₃₅₂₁, compared with FhbB₃₅₄₀₅, suggests potentially greater affinity for FH. To assess this possibility, surface plasmon resonance analyses were conducted and binding kinetics were measured. FhbB₃₃₅₂₁ bound FH with tighter affinity than FhbB₃₅₄₀₅ with K_D values of 0.90 and 1.51 μM , respectively. As discussed above, the tighter binding to FhbB₃₃₅₂₁ is most likely to be because of the more concentrated negative charge at the FH binding interface (refer to Fig. 5). The potential impact of this altered charge distribution is discussed in detail below.

Consistent with the extensive diversity between FhbB₃₅₄₀₅ and FhbB₃₃₅₂₁ these orthologs were found to be antigenically distinct from each other. Initial immunoblot analyses of r-FhbB proteins using antisera generated in mice against r-FhbB₃₅₄₀₅ revealed only weak detection of r-FhbB₃₃₅₂₁. To investigate this further, antisera to r-FhbB₃₅₄₀₅ and FhbB₃₃₅₂₁ (as individual proteins) were generated in rats and tested in immunoblot and IFA for their ability to detect r-FhbB₃₅₄₀₅ and FhbB₃₃₅₂₁. Antibody binding occurred strictly with the homologous protein. While the negatively charged $\alpha 1\alpha 2$ face of FhbB is the most divergent region of the protein, the positively charged face of the protein ($\beta 1\alpha 3\beta 2$) is well conserved and presumably surface exposed in the r-protein. Hence the absence of antibody in hyperimmune serum from both mice and rats that targets this face of the protein is somewhat surprising. FhbB has recently been proposed as a candidate for the development of a periodontal disease vaccine (McDowell *et al.*, 2012). It will be essential to further investigate and consider the antigenic diversity of FhbB in vaccine development efforts.

The presence of a spirochetal lipobox (Setubal *et al.*, 2006) in the FhbB sequence and the binding of FH to the surface of *T. denticola* (McDowell *et al.*, 2005) imply that FhbB is a surface-exposed lipoprotein. However, this has not been directly demonstrated. Surface exposure and membrane localization were assessed using IFA and Triton-X114 extraction

and phase partitioning approaches. Analyses by IFA using anti-FhbB antibody revealed uniform labeling and hence uniform distribution of FhbB on the cell surface. Consistent with the immunoblot analyses discussed above, efficient surface labeling using the anti-FhbB₃₅₄₀₅ and anti-FhbB₃₃₅₂₁ antiserum proved to be strain specific. The surface presentation demonstrated by IFA is consistent with Triton-X114 extraction and phase partitioning analyses that revealed that FhbB is amphipathic and concentrated in the detergent phase, properties consistent with it being an outer membrane lipoprotein.

The molecular basis of the interaction between FH and bacterial FH binding proteins has been intensively studied (Zipfel *et al.*, 2007; Lambris *et al.*, 2008; Ferreira *et al.*, 2010). Focusing on those produced by spirochetes, the majority interact with either CCP6–8 or CCP19–20 domains of FH (reviewed in McDowell *et al.*, 2012). The interaction site for FhbB₃₅₄₀₅ was previously localized to CCP6–8 (McDowell *et al.*, 2005). CCP7 is an important functional domain of FH that interacts with host-derived glycosaminoglycans and the inflammatory marker, CRP (Giannakis *et al.*, 2003; Hebecker *et al.*, 2010). Through a combination of modeling and mutational analyses, the FhbB₃₅₄₀₅ interaction site on FH has been mapped to CCP7. Collectively, the data presented here indicate that FhbB₃₃₅₂₁ interacts with CCPs 6 and 7 of FH. Mutational analyses were also conducted to identify residues of FhbB₃₃₅₂₁ that are involved in the FH binding interaction. Non-conservative substitutions at residues D45 and E58 abolished FH binding. Subtle differences in residues involved in FH binding exist between FhbB₃₅₄₀₅ and FhbB₃₃₅₂₁ as substitution of FhbB₃₅₄₀₅ E62 resulted in a loss of FH binding, whereas substitution of FhbB₃₃₅₂₁ D61 did not. It is noteworthy that in FhbB₃₅₄₀₅ the negative charge is more concentrated on a single helix, whereas in FhbB₃₃₅₂₁ the negative charge spans the termini of the two helices. With D61 at the edge of this negative charge pool, it is not surprising that its substitution had a minimal effect on FH binding. In FhbB₃₅₄₀₅, E62 is centrally located within the negatively charged FH binding interface presented by $\alpha 1\alpha 2$. Its substitution would interrupt the continuity of negative charge required for binding. The data presented support the hypothesis that structure and charge, as opposed to a strict primary amino acid sequence, are the dominant determinants in FH binding.

Dentilisin is an important virulence determinant that mediates several processes critical in *T. denticola* pathogenesis (Fenno *et al.*, 1998; Bian *et al.*, 2005; Bamford *et al.*, 2007; Miao *et al.*, 2011). As described here and in earlier reports, FhbB binds FH to the cell surface where it is then cleaved by dentilisin (McDowell *et al.*, 2009). Using a *T. denticola* strain 35405 dentilisin-deficient mutant (designated as CCE), we previously demonstrated that dentilisin is the sole protease responsible for FH cleavage (McDowell *et al.*, 2011). The ability, or lack thereof, of *T. denticola* strains to cleave FH could significantly influence the host–pathogen interaction and possibly the development, progression and severity of periodontal disease. There have been conflicting published reports regarding dentilisin activity of strain 33521 (Heuner *et al.*, 2001; Wyss *et al.*, 2004). Using the SAAPFNA cleavage assay, here we confirm a study that reported strain 33521 lacks dentilisin activity (Wyss *et al.*, 2004). Consistent with this, when purified human FH was incubated with strain 33521, cleavage was not observed. Hence, *in vivo*, various strains of *T. denticola* may not participate in FH cleavage.

It stands to reason that *T. denticola* strains deficient in dentilisin activity would be more efficient in evading complement mediated killing. Using 33521 as an example, this strain binds FH with higher affinity and because it does not cleave FH, bound FH would be retained at the cell surface longer. Consistent with this hypothesis strain 33521, which does not cleave FH, was slightly more serum resistant than 35405. The dentilisin-deficient phenotype could be beneficial for *T. denticola* in a healthy subgingival crevice before the onset of active periodontal disease. In such an environment the ability to evade complement-mediated killing would facilitate low-level persistence. As periodontal disease begins to develop and the relative numbers of *T. denticola* increase, immune evasion may become less important because of the physical protection provided by the highly developed oral biofilm. The possible proliferation of *T. denticola* strains that cleave FH in periodontal pockets could lead to local FH depletion. In the absence of sufficient FH, immune dysregulation would occur. Specifically factor I-mediated cleavage of C3b and decay of the C3bBb convertase complex would be inhibited, resulting in accumulation of C3b on host cells. Deposition of C3b on host cells would disrupt normal self-recognition mechanisms and lead to destruction of the

periodontium. Local FH depletion could also impact regulation of the classical complement cascade. Factor H has been demonstrated to bind to mCRP. C-reactive protein is highly elevated in patients with periodontal disease (Gomes-Filho *et al.*, 2011). The FH–mCRP complex functions to negatively regulate the C5 convertase complex on apoptotic cell surfaces to allow for clearance of damaged cells in a controlled mechanism, limiting immune activation (Mihlan *et al.*, 2009). In the absence of such regulation there would be a significant increase in membrane attack complex formation and further cellular damage. There would also be an increase in the potent anaphylatoxin C5a resulting in the production of proinflammatory cytokines and inhibited clearance of damaged cells. Hence if FH were limiting, tissue repair would be inefficient while inflammation and tissue destruction would ensue. Interestingly, one of the binding sites on FH for mCRP is within CCP7 (Giannakis *et al.*, 2003; Okemefuna *et al.*, 2010; Perkins *et al.*, 2010a, b) which is the binding site for the *T. denticola* FhbB protein (this study; McDowell *et al.*, 2005). It remains to be determined if FhbB competes with CRP for binding to FH. The affinity of the CRP–FH interaction has been determined to be 4.2 μM (Okemefuna *et al.*, 2010), weaker than the FhbB–FH interaction (Miller *et al.*, 2012) indicating that FhbB could competitively inhibit CRP binding to FH.

The periopathogen community may benefit from FH depletion through several different mechanisms. First, enlargement of periodontal pockets as a result of immune-mediated destruction would expand the anaerobic environment and promote growth of periopathogens, which are mostly strict anaerobes. In addition, the destruction of tissue would release nutrients that promote growth.

There is much to be learned about the interplay between periopathogens and the host immune system. The local degradation of immune regulatory molecules by some members of the periopathogen community may prove to be a key driving force in disease progression. It has recently been suggested that *Porphyromonas gingivalis* also subverts the host immune response in a manner that favors the growth of periopathogens (Hajishengallis, 2011; Hajishengallis *et al.*, 2011, 2012). Intervention strategies that disrupt these pathogen-induced host damaging processes may offer novel non-invasive approaches to controlling periodontal disease.

ACKNOWLEDGEMENTS

This study was supported in part by grants from NIDCR to R.T.M. (DE017401), NIDCR to D.P.M. (F31DE023000), NIH/NIAID for A.A. and M.J.C. (AI29735 and AI085248), NIH/NIGMS for M.J.C. (GM072004) and by NIH grants (P30CA160859) to the VCU Flow Cytometry Core.

REFERENCES

- Bamford, C.V., Fenno, J.C., Jenkinson, H.F. and Dymock, D. (2007) The chymotrypsin-like protease complex of *Treponema denticola* ATCC 35405 mediates fibrinogen adherence and degradation. *Infect Immun* **75**: 4364–4372.
- Beck, J.D. (1987) Public health dentistry: planning for the future. *J Public Health Dent* **47**: 26–30.
- Bian, X.L., Wang, H.T., Ning, Y., Lee, S.Y. and Fenno, J.C. (2005) Mutagenesis of a novel gene in the *prcA*-*prtP* protease locus affects expression of *Treponema denticola* membrane complexes. *Infect Immun* **73**: 1252–1255.
- Boackle, R.J. (1991) The interaction of salivary secretions with the human complement system—a model for the study of host defense systems on inflamed mucosal surfaces. *Crit Rev Oral Biol Med* **2**: 355–367.
- Boackle, R.J., Pruitt, K.M., Silverman, M.S. and Glymph, J.L. Jr (1978) The effects of human saliva on the hemolytic activity of complement. *J Dent Res* **57**: 103–110.
- Chen, V.B., Arendall, W.B., Headd, J.J. *et al.* (2010) MolProbity: all-atom structure validation for macromolecular crystallography. *Acta Crystallogr D Biol Crystallogr* **66**: 12–21.
- Darveau, R.P. (2010) Periodontitis: a polymicrobial disruption of host homeostasis. *Nat Rev Microbiol* **8**: 481–490.
- Davis, I.W., Leaver-Fay, A., Chen, V.B. *et al.* (2007) MolProbity: all-atom contacts and structure validation for proteins and nucleic acids. *Nucleic Acids Res* **35**: W375–W383.
- Earnhart, C.G., Buckles, E.L. and Marconi, R.T. (2007) Development of an *OspC*-based tetravalent, recombinant, chimeric vaccinogen that elicits bactericidal antibody against diverse Lyme disease spirochete strains. *Vaccine* **25**: 466–480.
- Ellen, R.P. and Galimanas, V.B. (2005) Spirochetes at the forefront of periodontal infections. *Periodontology* **2000** (38): 13–32.
- Fenno, J.C. (2012) *Treponema denticola* interactions with host proteins. *J Oral Microbiol* doi: 10.3402/jom.v4i0.9929.
- Fenno, J. and McBride, B. (1998) Virulence factors of oral treponemes. *Anaerobe* **4**: 1–17.
- Fenno, J.C., Hannam, P.M., Leung, W.K., Tamura, M., Uitto, V.J. and McBride, B.C. (1998) Cytopathic effects of the major surface protein and the chymotrypsinlike protease of *Treponema denticola*. *Infect Immun* **66**: 1869–1877.
- Ferreira, V.P., Pangburn, M.K. and Cortes, C. (2010) Complement control protein factor H: the good, the bad, and the inadequate. *Mol Immunol* **47**: 2187–2197.
- Giannakis, E., Jokiranta, T.S., Male, D.A. *et al.* (2003) A common site within factor H SCR 7 responsible for binding heparin, C-reactive protein and streptococcal M protein. *Eur J Immunol* **33**: 962–969.
- Goetting-Minesky, M.P., Godovikova, V., Li, J.J. *et al.* (2012) Conservation and revised annotation of the *Treponema denticola* *prcB*-*prcA*-*prtP* locus encoding the dentilisin (CTLP) protease complex. *Mol Oral Microbiol* **28**: 181–191.
- Gomes-Filho, I.S., Freitas Coelho, J.M., da Cruz, S.S. *et al.* (2011) Chronic periodontitis and C-reactive protein levels. *J Periodontol* **82**: 969–978.
- Hajishengallis, G. (2011) Immune evasion strategies of *Porphyromonas gingivalis*. *J Oral Biosci* **53**: 233–240.
- Hajishengallis, G., Liang, S., Payne, M.A. *et al.* (2011) Low-abundance biofilm species orchestrates inflammatory periodontal disease through the commensal microbiota and complement. *Cell Host Microbe* **10**: 497–506.
- Hajishengallis, G., Krauss, J.L., Liang, S., McIntosh, M.L. and Lambris, J.D. (2012) Pathogenic microbes and community service through manipulation of innate immunity. *Adv Exp Med Biol* **946**: 69–85.
- Hebecker, M., Okemefuna, A.I., Perkins, S.J., Mhlan, M., Huber-Lang, M. and Jozsi, M. (2010) Molecular basis of C-reactive protein binding and modulation of complement activation by factor H-related protein 4. *Mol Immunol* **47**: 1347–1355.
- Heuner, K., Bergmann, I., Heckenbach, K. and Gobel, U.B. (2001) Proteolytic activity among various oral *Treponema* species and cloning of a *prtP*-like gene of *Treponema socranskii* subsp. *socranskii*. *FEMS Microbiol Lett* **201**: 169–176.
- Hovis, K.M., McDowell, J.V., Griffin, L. and Marconi, R.T. (2004) Identification and characterization of a linear-plasmid-encoded factor H-binding protein (FhbA) of the relapsing fever spirochete *Borrelia hermsii*. *J Bacteriol* **186**: 2612–2618.
- Hovis, K.M., Freedman, J.C., Zhang, H., Forbes, J.L. and Marconi, R.T. (2008) Identification of an antiparallel coiled-coil/loop domain required for ligand binding by

- the *Borrelia hermsii* FhbA protein: additional evidence for the role of FhbA in the host-pathogen interaction. *Infect Immun* **76**: 2113–2122.
- Jarva, H., Jokiranta, T.S., Hellwage, J., Zipfel, P.F. and Meri, S. (1999) Regulation of complement activation by C-reactive protein: Targeting then complement regulatory activity of factor H by an interaction with short consensus repeat domains 7 and 8–11. *J Immunol* **163**: 3957–3962.
- Lambris, J.D., Ricklin, D. and Geisbrecht, B.V. (2008) Complement evasion by human pathogens. *Nat Rev Microbiol* **6**: 132–142.
- Larkin, M.A., Blackshields, G., Brown, N.P. *et al.* (2007) Clustal W and Clustal X version 2.0. *Bioinformatics* **23**: 2947–2948.
- Loesche, W.J. (1988) The role of spirochetes in periodontal disease. *Adv Dent Res* **2**: 275–283.
- McDowell, J.V., Sung, S.Y., Hu, L.T. and Marconi, R.T. (2002) Evidence that the variable regions of the central domain of VlsE are antigenic during infection with Lyme disease spirochetes. *Infect Immun* **70**: 4196–4203.
- McDowell, J.V., Lankford, J., Stamm, L., Sadlon, T., Gordon, D.L. and Marconi, R.T. (2005) Demonstration of factor H-like protein 1 binding to *Treponema denticola*, a pathogen associated with periodontal disease in humans. *Infect Immun* **73**: 7126–7132.
- McDowell, J.V., Frederick, J., Stamm, L. and Marconi, R.T. (2007) Identification of the gene encoding the FhbB protein of *Treponema denticola*, a highly unique factor H-like protein 1 binding protein. *Infect Immun* **75**: 1050–1054.
- McDowell, J. V., Huang, B., Fenno, J. C. and Marconi, R.T. (2009) Analysis of a unique interaction between the complement regulatory protein factor H and the periodontal pathogen *Treponema denticola*. *Infect Immun* **77**: 1417–1425.
- McDowell, J.V., Frederick, J., Miller, D.P. *et al.* (2011) Identification of the primary mechanism of complement evasion by the periodontal pathogen, *Treponema denticola*. *Mol Oral Microbiol* **26**: 140–149.
- McDowell, J.V., Miller, D.P., Mallory, K.L. and Marconi, R.T. (2012) *Treponema denticola*: FhbB, Dentilisin, Complement Evasion and the Paradox of Factor H Cleavage. In: Embers M.E. ed. *The Pathogenic Spirochetes: Strategies for Evasion of Host Immunity and Persistence*. New York: Springer Science+Business Media, pp. 43–62.
- Miao, D., Fenno, J.C., Timm, J.C., Joo, N.E. and Kapila, Y.L. (2011) The *Treponema denticola* chymotrypsin-like protease dentilisin induces matrix metalloproteinase-2-dependent fibronectin fragmentation in periodontal ligament cells. *Infect Immun* **79**: 806–811.
- Mihlan, M., Stippa, S., Jozsi, M. and Zipfel, P.F. (2009) Monomeric CRP contributes to complement control in fluid phase and on cellular surfaces and increases phagocytosis by recruiting factor H. *Cell Death Differ* **16**: 1630–1640.
- Miller, D.P., McDowell, J.V., Bell, J. K. and Marconi, R.T. (2011) Crystallization of the factor H-binding protein, FhbB, from the periodontal pathogen *Treponema denticola*. *Acta Crystallogr Sect F Struct Biol Cryst Commun* **67**: 678–681.
- Miller, D.P., Bell, J.K., McDowell, J.V. *et al.* (2012) Structure of factor H binding protein B (FhbB) of the periodontal pathogen, *Treponema denticola*: Insights into the progression of periodontal disease. *J Biol Chem* **287**: 12715–12722.
- Okemefuna, A.I., Nan, R., Miller, A., Gor, J. and Perkins, S.J. (2010) Complement factor H binds at two independent sites to C-reactive protein in acute phase concentrations. *J Biol Chem* **285**: 1053–1065.
- Paster, B.J., Olsen, I., Aas, J.A. and Dewhirst, F.E. (2006) The breadth of bacterial diversity in the human periodontal pocket and other oral sites. *Periodontol* **42**: 80–87.
- Perkins, S.J., Nan, R., Okemefuna, A.I., Li, K., Khan, S. and Miller, A. (2010a) Multiple interactions of complement Factor H with its ligands in solution: a progress report. *Adv Exp Med Biol* **703**: 25–47.
- Perkins, S.J., Okemefuna, A.I. and Nan, R. (2010b) Unravelling protein-protein interactions between complement factor H and C-reactive protein using a multidisciplinary strategy. *Biochem Soc Trans* **38**: 894–900.
- Roberts, D.M., Theisen, M. and Marconi, R.T. (2000) Analysis of the cellular localization of Bdr paralogs in *Borrelia burgdorferi*, a causative agent of Lyme disease: evidence for functional diversity. *J Bacteriol* **182**: 4222–4226.
- Ruddy, S. and Austen, K.F. (1969) Hemolytic measurement by the inactivation of cell-bound C3. *J Immunol* **102**: 533–543.
- Ruddy, S. and Austen, K.F. (1971) C3b inactivator of man. II. Fragments produced by C3b inactivator cleavage of cell-bound or fluid phase C3b. *J Immunol* **107**: 742–750.
- Sali, A. (1995) Comparative protein modeling by satisfaction of spatial restraints. *Mol Med Today* **1**: 270–277.
- Sali, A., Potterton, L., Yuan, F., van Vlijmen, H. and Karplus, M. (1995) Evaluation of comparative protein modeling by MODELLER. *Proteins* **23**: 318–326.

- Schenkein, H.A. (1991) The role of complement in periodontal diseases. *Crit Rev Oral Biol Med* **2**: 65–81.
- Schenkein, H.A. and Genco, R.J. (1977) Gingival fluid and serum in periodontal diseases. I. Quantitative study of immunoglobulins, complement components, and other plasma proteins. *J Periodontol* **48**: 772–777.
- Setubal, J.C., Reis, M., Matsunaga, J. and Haake, D.A. (2006) Lipoprotein computational prediction in spirochaetal genomes. *Microbiology* **152**: 113–121.
- Simonson, L.G., Goodman, C.H., Bial, J.J. and Morton, H.E. (1988) Quantitative relationship of *Treponema denticola* to severity of periodontal disease. *Infect Immun* **56**: 726–728.
- Socransky, S., Haffajee, A., Cugini, M., Smith, C. and Kent, R.J. (1998) Microbial complexes in subgingival plaque. *J Clin Periodontol* **25**: 134–144.
- Uitto, V.J., Grenier, D., Chan, E.C. and McBride, B.C. (1988) Isolation of a chymotrypsinlike enzyme from *Treponema denticola*. *Infect Immun* **56**: 2717–2722.
- Wyss, C., Moter, A., Choi, B.K. *et al.* (2004) *Treponema putidum* sp. nov., a medium-sized proteolytic spirochaete isolated from lesions of human periodontitis and acute necrotizing ulcerative gingivitis. *Int J Syst Evol Microbiol* **54**: 1117–1122.
- Zipfel, P.F. and Skerka, C. (2009) Complement regulators and inhibitory proteins. *Nat Rev Immunol* **9**: 729–740.
- Zipfel, P.F., Skerka, C., Hellwage, J. *et al.* (2002) Factor H family proteins: on complement, microbes and human diseases. *Biochem Soc Trans* **30**: 971–978.
- Zipfel, P.F., Wurzner, R. and Skerka, C. (2007) Complement evasion of pathogens: common strategies are shared by diverse organisms. *Mol Immunol* **44**: 3850–3857.
- Zipfel, P.F., Hallstrom, T., Hammerschmidt, S. and Skerka, C. (2008) The complement fitness factor H: role in human diseases and for immune escape of pathogens, like pneumococci. *Vaccine* **26**(Suppl 8): I67–I74.

Copyright of Molecular Oral Microbiology is the property of Wiley-Blackwell and its content may not be copied or emailed to multiple sites or posted to a listserv without the copyright holder's express written permission. However, users may print, download, or email articles for individual use.